Research Paper

Amycolatopsis sp. strain MN235945 Mediated Biosynthesis of Silver Nanoparticles: Characterization, Antimicrobial and Anticancer Activity against HeLa and MCF-7 Cell Lines

PALLAVI SATHYANARAYANA SWAMY, M. P. BHAT AND S. NAYAKA*

Department of Botany, Karnatak University, Dharwad, Karnataka 580003, India

Swamy *et al.*: Anticancer activity of *Amycolatopsis* sp. mediated Silver Nanoparticles

The current study investigated about the biogenic synthesis and evaluation of biological activities of *Amycolatopsis* sp. strain MN235945 fabricated silver nanoparticles and their characterization by ultraviolet-visible spectroscopy, fourier transform infrared spectroscopy, high resolution-transmission electron microscopy, energy dispersive X-ray spectroscopy, X-ray diffractometry and zeta potential analysis. The most potent isolate *Amycolatopsis* sp. strain MN235945 was identified by morphological and genotypic characterization and biological activity of silver nanoparticles was studied *via* antimicrobial and anticancer activity assays. The synthesized silver nanoparticles with spherical shape and polydispersed nature showed ultraviolet visible spectroscopy, absorption maximum at 417 nm with the smallest size of 19.40 nm. The presence of various biological functional groups and different elemental composition of silver nanoparticles were determined along with zeta potential value of -34.8 mV; whereas, the X-ray diffractometry analysis revealed the specific Bragg's diffraction peaks for metallic silver. The silver nanoparticles with increased antimicrobial activity significantly inhibited cervical adenocarcinoma HeLa and human breast cancer MCF-7 tumour cells with IC_{50} values of 81.12 and 235.45 µg/ml respectively. These encouraging results obtained *via* low-cost green synthesis of silver nanoparticles from marine *Amycolatopsis* sp. strain MN235945 provide helpful information for further research and designing an anticancer agent in coming years using *Amycolatopsis* sp. strain MN235945 mediated silver nanoparticles with minimal side effects.

Key words: Marine *Amycolatopsis* sp., silver nanoparticles, antimicrobial, anticancer activity, reactive oxygen species

Nanotechnology is an essential field in recent days, where it is dealing with many research like synthesis, characterization and different shapes, sizes (1-100 nm) of the nanoparticles. Several studies regarding the synthesis of biological nanoparticles using various microorganisms like fungi, Actinomycetes, bacteria, viruses and different plant parts are investigated. It shows promising potential for controlling different pathogens. With multiple applications, nanoparticle research plays a vital role in the fields such as cancer study[1], larvicidal and insecticidal activity[2] and plant disease control in agricultural sciences[3]. Biological activities like antibacterial, antifungal, anticancer[4], anti-inflammatory, antiviral, cardioprotection[5], wound healing[6], and biosurfactants[7] helped nanotechnology to gain enormous popularity within a short time.

Silver nanoparticles (AgNPs) have been used in various applications like cosmetics, solar cells, catalysts, ceramics, gas sensors, anti-bacterial properties, energy sector plastics, environmental protection[8], drug delivery and bioimaging, textiles, probes, commercial products such as pastes, food packaging, soaps, optical and electrical properties, toxicity against cancer cells[9,10]. There are varieties of methods like physical, chemical and biological approaches to synthesize AgNPs and biological synthesis of AgNPs is more opted[11,12]. The AgNPs synthesis using various microorganisms are well documented in *Streptomyces rochei* MHM13[13], *Aspergillus tamarii*[14], *Penicillium atramentosum* KM[15], *Acinetobacter baumannii*[16], *Gordonia amicalis* HS11[17], and *Escherichia coli*[18], *Lactobacillus plantarum* TA4[19] and from *Enhalus acoroides*[20].

***Address for correspondence**
E-mail: sreenivasankud@gmail.com

Accepted 15 September 2022
Revised 11 December 2021
Received 20 July 2021
Indian J Pharm Sci 2022;84(5):1178-1188

Actinomycetes are unicellular, gram-positive bacteria; it belongs to the order Actinomycetales. This group is widely distributed in the environment and found in various habitats like plants, soil, freshwater, marine, and soil, etc. and well known for producing many antibiotics. The present investigation focuses upon the formation of AgNPs by *Amycolatopsis* sp. which is a reducing agent. *Amycolatopsis* sp. has many antibiotics like balhimycin, tolypomycin, vancoresmycin and nogabecin[21].

In present days, cancer is among the reasons for the highest number of mortality worldwide, as mentioned in one out of six deaths across the globe[22]. Among the various types of cancers in humans, cervical and breast carcinoma are observed in the highest percentage of incidence[21]. These cells spread in the blood and lymph system through the entire body; despite chemotherapy, radiotherapy is the most common type of cancer treatment, these protocols causing side effects. These advantages are cost-effective for the synthesis of nanoparticles for cancer treatment. At present, AgNPs are used as anticancer agents to treat several types of cancers such as epithelial carcinoma (A549), hepatocellular carcinoma (HepG2)[23], cervical adenocarcinoma (HeLa)[24] and human breast cancer (MCF-7)[25].

Meanwhile, AgNPs have been recognized as innovative materials and have found their applications in different fields, starting from antimicrobials to cancer therapy[26]. The present study is carried out for the first time using *Amycolatopsis* sp. strain MN235945 for the synthesis of AgNPs and their cytotoxic activity against HeLa and MCF-7 cell lines.

MATERIALS AND METHODS

Sample collection and isolation of Actinomycetes:

The sediment samples were collected from different locations of Maravanthe beach, Kundapur, Udupi, Karnataka, India. The samples were used to isolate Actinomycetes on starch casein agar media using the spread plate method. Later, the pure cultures of Actinomycetes strains were screened for antagonistic activities by perpendicular streak method and the isolate showing good inhibition activity was selected for AgNPs synthesis.

Preparation of cell free extract and biosynthesis of AgNPs:

The isolated marine Actinomycetes were cultured in a 250 ml conical flask containing 100 ml of starch casein broth medium at pH 7.2 with the following composition starch 1 g, casein 0.03 g, calcium carbonate 0.002 g, ferrous sulphate 0.001 g, potassium nitrate 0.2 g, magnesium sulphate 0.005 g and sodium chloride 0.2 g. The incubation of the inoculated flasks was done at 33° for 5 d. After incubation, cultures were centrifuged at 8000 RPM for 15 min to obtain the culture supernatant and the same was mixed with an aqueous solution of 1 mM silver nitrate (100 ml) at pH 8.0. The mixture was incubated in the dark for 5 d to allow the formation of AgNPs and observed for the colour change in the reaction mixture.

Characterization of synthesized AgNPs:

The bio-reduction of silver ions (Ag^+) to elemental silver (Ag^0) was monitored in the scanning range between 300 to 700 nm by using a double beam Ultra-Violet Visible (UV-Vis) spectrophotometer (METASHUV-9000 A). The Fourier-Transform Infrared (FTIR) spectroscopy was performed to detect possible bio-reductants by scanning in the range of 4000 to 400 cm^{-1} with 4 cm^{-1} resolution using FTIR instrument (Nicolet 6700, USA). The AgNPs were observed under Scanning Electron Microscope (SEM) equipped with Energy Dispersive X-Ray (EDX) analyzer (JSM-IT 500LA) to determine morphology and elemental composition. The shape and size of the biosynthesized AgNPs were determined by High Resolution Transmission Electron Microscopic (HR-TEM) analysis (FEI, TECNAI G2, F30) with an accelerating voltage of 100 kV. The particle size and surface morphology of nanoparticles were evaluated using Image J 1.45 software. The crystal structure and particle size were studied by X-Ray Diffraction (XRD) (Rigaku Miniflex Smart Lab SE, 600) instrument and operating at 40 kV and 30 mA. The size and surface charge values were measured with the help of the zeta potential instrument (Horiba Scientific) and the thermal stability of AgNPs was studied by Thermo-Gravimetric Analysis (TGA) from room temperature to 600° using TGA instrument (TA instruments, SDT Q 600 and DSC Q20, USA).

Genotypic characterization of potent isolate:

Genomic DNA was isolated from the selected strain and 16S rRNA genes were amplified and sequenced using the Sanger sequencing method (Applied Biosystems, 3500 series genetic analyzer). The obtained gene sequence was deposited to the National Center for Biotechnology Information database *via* nucleotide BLAST (BLASTn) web portal. The DNA sequence

was aligned and the taxonomical hierarchy was studied by constructing neighbour joining the phylogenetic tree using MegAlign Pro 17 (DNASTAR Lasergene) software.

Antimicrobial activity of AgNPs:

Antimicrobial activity of AgNPs fabricated by *Amycolatopsis* sp. strain MN235945 was tested against pathogenic microorganisms like *Pseudomonas aeruginosa* (MTCC424), *Staphylococcus aureus* (MTCC6908), *Enterococcus faecalis* (MTCC6845), *Escherichia coli* (MTCC40), *Fusarium oxysporum* (MTCC2087), *Candida glabrata* (MTCC3814), *Alternaria alternata* (MTCC2060) and *Candida albicans* (MTCC227) were procured from National Collection for Industrial Microorganisms, Pune, India and sub-cultured on nutrient broth media before incubating at 37° for 48 h. For the agar well diffusion method, the bacterial and fungal cultures were spread on Mueller-Hinton agar plate using a sterile cotton swab. The wells were loaded with 25, 50, 75, 100 µl of AgNPs suspension (1 mg/ml stock) and 50 µl of distilled water was used as negative control; whereas 50 µl of (25 µg/ml) streptomycin and fluconazole were taken as standards for bacteria and fungi, respectively.

Evaluation of Minimum Inhibitory Concentration (MIC) and Minimum Bactericidal Concentration (MBC):

The inhibitory action of AgNPs was further tested using MIC and MBC studies on bacterial pathogens to find out the minimum concentration of AgNPs that inhibit the growth of bacterial strains. The tests were carried out according to the methods described in Clinical and Laboratory Standards Institute (CLSI) and conducted on 96-well microtiter plates for MIC by taking resazurin as indicator with streptomycin as standard; and the MBC test was conducted on Mueller-Hinton agar plates. For MIC the bacterial inoculum concentration of 10^6 Mcfarland standards was taken along with 100 µl of AgNPs (500 µg/ml) from the stock solution.

Column 1 with only medium and column 2 with medium and bacterial inoculum were taken as negative and positive controls, respectively. Further, 30 µl of resazurin was added in each well and the plate was incubated at 37° for 24 h. Similarly, the MBC test was performed by spreading the suspension from each well of microtiter plate on Mueller-Hinton agar plates and incubated at 37° for 48 h. Finally, the concentration at which the bacterial growth was not observed was taken as MIC and MBC values.

***In vitro* anticancer activity of AgNPs:**

Cell viability (3-(4, 5-dimethylthiazolyl-2)-2, 5-diphenyltetrazolium bromide (MTT)) assay: The cytotoxicity of AgNPs was tested against HeLa and MCF-7 cell lines using MTT cell viability assay. The cancer cell lines were procured from the National Centre for Cell Science, Pune, India, and sub-cultured on Dulbecco Modified Eagle Medium (DMEM- #AL111, Himedia). Both cancer cell lines were separately plated in 96 well plates (Corning, USA) at a density of 20 000 cells per well without AgNPs (control). The cells were allowed to grow for 24 h inside a 5 % CO_2 incubator (Healforce, China), and then the desired concentrations of AgNPs (6.25, 12.5, 25, 50 and 100 µg/ml) were added along with 0.5 mg/ml of MTT reagent (#4060, Himedia) and 4.3 µg/ml (HeLa) and 3.48 µg/ml (MCF-7) camptothecin (#C9911, Sigma) as standard. After incubating for 24 h at 37° in a 5 % CO_2 atmosphere, the spent media was removed from the plates. Further, 100 µl of Dimethyl Sulfoxide (DMSO- #PHR1309, Sigma) was added after removing the MTT reagent. The absorbance was read on an Enzyme Linked Immunosorbent Assay (ELISA) reader to determine the change in colour intensity at 570 nm using 630 nm as a reference wavelength.

Reactive Oxygen Species (ROS) assay: HeLa and MCF-7 cells were cultured on DMEM medium in a 96-well plate with 10 000 cells/200 µl cell density and incubated in a CO_2 incubator at 37° for 24 h. The spent medium was aspirated and washed with 100 µl of 1X Phosphate Buffer Saline (PBS) and then treated with H_2O_2 of 100 µM concentration and test compounds with IC_{50} concentrations except for cell control in 200 µl of culture medium before keeping the cells for 24 h incubation.

Then, the medium was removed and washed with PBS. For staining, 2',7'-dichlorodihydrofluorescein diacetate (H2DCFDA) stock solution (4 mM) was diluted into Dulbecco's Phosphate Buffered Saline (DPBS, #TL1006, Himedia) to make 10 µM fresh working solution. Finally, the cells were stained with H2DCFDA and kept for incubation for 2 h at 37° under dark. Further, the cells were observed under a confocal microscope at different time intervals (0 to 120 min) at excitation and emission wavelengths of 488 nm and 535 nm, and images were analyzed by Image J software and recorded.

RESULTS AND DISCUSSION

The green synthesis of AgNPs by *Amycolatopsis* sp. strain MN235945 was primarily indicated by the colour change of the reaction mixture from colourless to brown after adding $AgNO_3$. The UV-Vis spectrum showed an absorption maximum at 417 nm after the incubation period confirming the synthesis of biogenic AgNPs (fig. 1A and fig. 1B). The previous studies reported that the change in the colour of the reaction mixture after adding $AgNO_3$ was due to the excitation of surface plasmon resonance phenomenon of metallic silver. Further, AgNPs synthesis was confirmed by UV-Vis. spectrum because of the optic response of AgNPs of marine *Streptomyces rochei* MHM13 and *Streptomyces* sp. GUT 21 indicated a strong surface plasmon resonance band at 410 nm[13,27].

The FTIR spectrum of AgNPs revealed absorption bands at 3290, 2930, 1726, 1635, 1351, 1026, 823, 463 and 429 cm^{-1}, respectively (fig. 2). The strong intensity band at 3290 cm^{-1} was characteristic of O=H bonded alcohols, and the strong, intensive peak at 2930 cm^{-1} corresponded to C-H stretching alkanes. Similarly, the band at 1726 cm^{-1} was attributed to C=O aldehyde; 1635 cm^{-1} to N-H bending primary and secondary amines, and the peak at 1351 cm^{-1} corresponded to S=O sulfones, sulfates, and sulfonyl chlorides. The medium intensity peak at 1026 cm^{-1} assigned to the C-O bonded ethers, esters, and carboxylic acids. The weak intensity peak at 823 cm^{-1} was correlated to C-H bending aromatics, and the other weak intensity peak at 463 cm^{-1} corresponded to C-X bonded bromide or iodide. Similar results were observed stating the role of biological materials in the reduction and synthesis of AgNPs, where proteins and other biomaterials were present along with AgNPs as capping and stabilization components. Also the data indicated that amines, alcohols, alkanes, alkynes, amino acids, and carboxylates residues involved in the synthesis, capping and stabilization of AgNPs[28,29].

The biosynthesized AgNPs were elucidated with HR-TEM to determine the surface morphology and size of the AgNPs. HR-TEM micrograph showed polydispersed, spherical-shaped AgNPs with the smallest size of 19.40 nm (fig. 3A). The previous studies on HR-TEM analysis of biosynthesized AgNPs from *Streptomyces* sp. and *Nocardiopsis alba* supported our results, where the synthesized AgNPs size ranged from 10 to 20 nm and 20 to 60 nm, respectively. The synthesis of AgNPs from microbes depends on the concentration of metal ions and incubation period provided[30,31].

The elemental composition of *Amycolatopsis* sp. strain MN235945 synthesized AgNPs was obtained by EDX analysis. An intense signal at 3 keV in the metallic silver region was observed as the confirmation for the AgNPs synthesis. EDX determines the abundance and distribution of specific elements present in the nanoparticles. A trace elemental mapping of AgNPs by EDX pattern was obtained for Carbon (C) (40.09 %), Oxygen (O) (38.72 %), Sodium (Na) (3.34 %), Chlorine (Cl) (5.67 %), Potassium (K) (1.82 %), and Silver (Ag) (10.37 %), as shown in fig. 3B. The strong signal energy peaks in the range of 2 to 4 keV. Similar results suggested about metallic AgNPs, which typically depicted a strong signal peak at 3 keV due to surface plasmon resonance and the weaker signals for C, O, K, and silicon, the other biomolecules that are involved in the capping of AgNPs. They also suggested that, among the different signals, the C, K and other signals may probably be due to X-ray emission from proteins, enzymes, and carbohydrates in extracts[32,33].

X-ray diffraction analysis of *Amycolatopsis* sp. strain MN235945 synthesized AgNPs revealed well-defined peaks for metallic crystal silver with the crystalline nature of AgNPs. The XRD pattern showed the main reflection planes at the 2Θ degrees of 32.16°, 46.13°, 57.36° and 76.60° respectively, corresponding to the (111), (200), (220), and (311) facets of the Bragg's planes, suggesting the Face-Centered Cubic (FCC) nature (fig. 3C). Similarly, the XRD data showed that the AgNPs fabricated by endophytic Actinomycetes showed particle size from 19 to 35 nm with the peaks indicating the Bragg's scattering of crystalline AgNPs with spiral structures and depicted the crystalline nature of the synthesized AgNPs[34,35].

The stability of the biosynthesized AgNPs was analyzed by zeta potential peak at -34.8 mV (fig. 3D), which suggested that the surface of the AgNPs was negatively charged and well dispersed in the medium. The higher negative values indicated higher stability of AgNPs, and zeta analysis indicated the high dispersivity and well-defined colloidal nature of the AgNPs. The obtained results agreed with the previous study, which also reported higher negative values of zeta potential and these values confirmed the repulsion among the particles and proved that they were very stable[36].

The genomic DNA was extracted from the isolated strain, and the 16S rRNA was amplified with the help of 27F forward (5'-AGAGTTTGATCCTGGCTCAG-3') and 1492R reverse (5'-GGTTACCTTGTTACGACTT-3') primer.

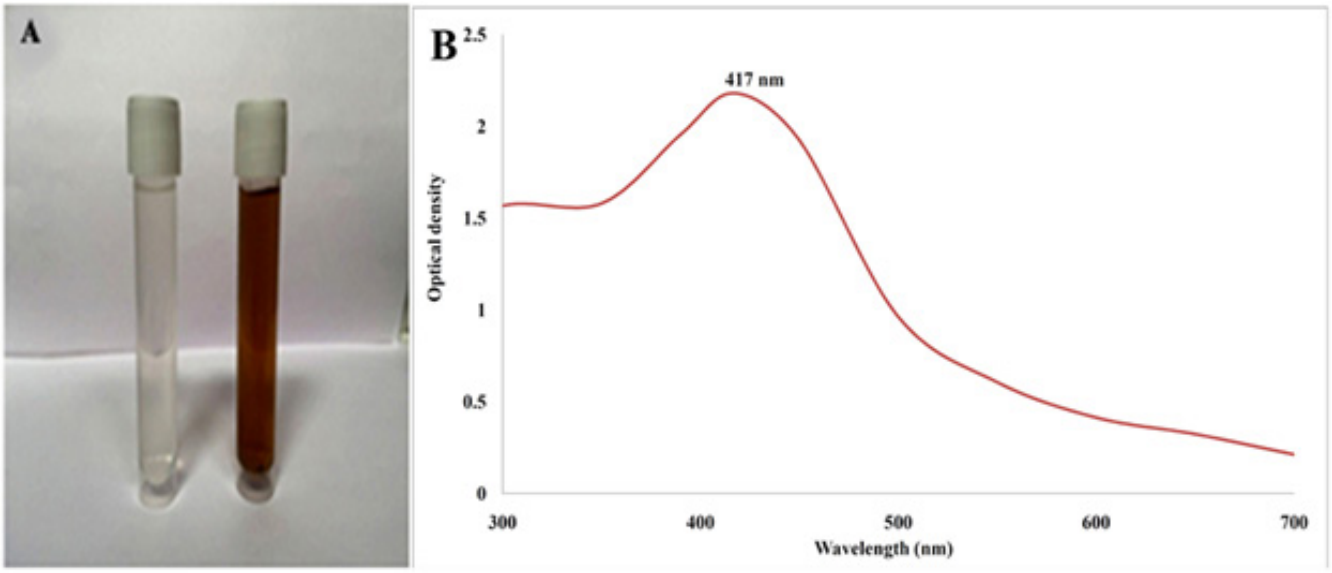

Fig. 1: (A) Visual observation of colour of reaction mixture before and after synthesis; (B) UV-Vis. absorption spectrum of AgNPs synthesized by *Amycolatopsis* sp. strain MN235945

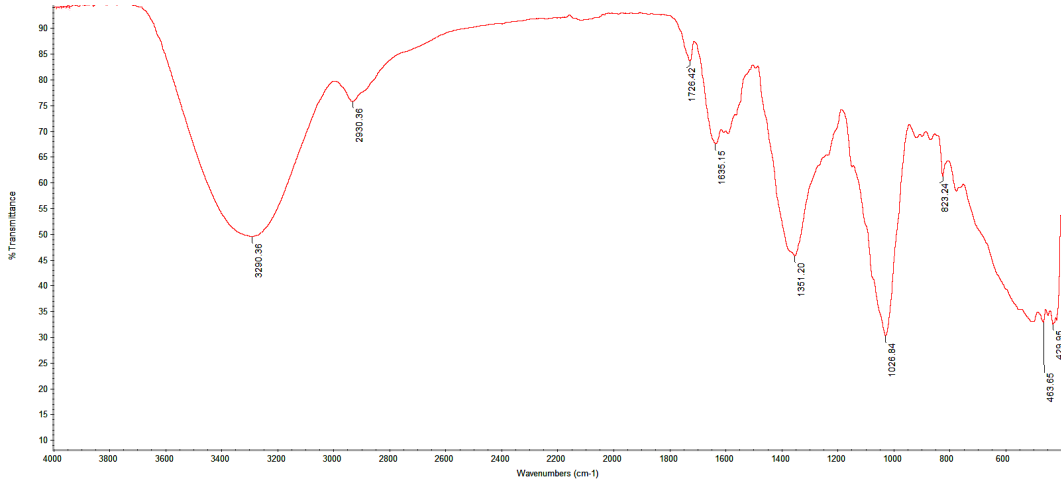

Fig. 2: FTIR spectrum analysis of AgNPs synthesized by *Amycolatopsis* sp. strain MN235945

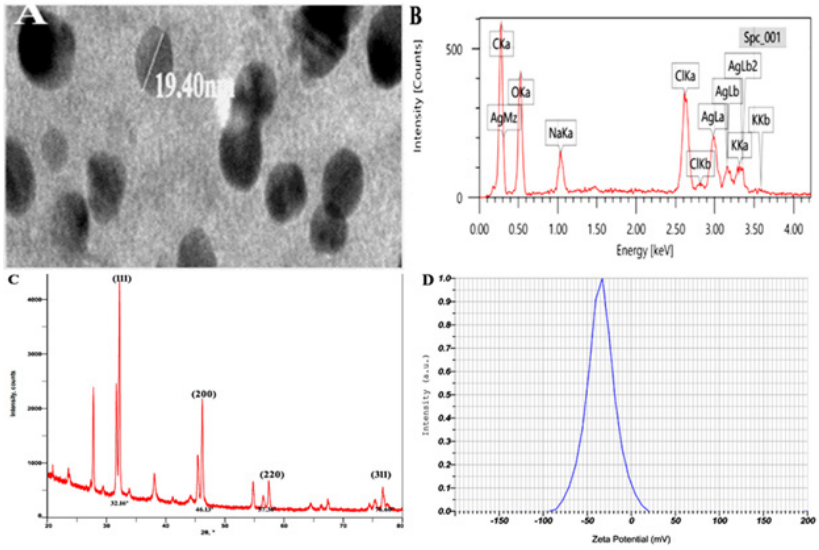

Fig. 3: Characterization of *Amycolatopsis* sp. strain MN235945 AgNPs; (A): HR-TEM; (B): EDX; (C): XRD and (D): Zeta potential

The genomic 16S rDNA and the amplified 16S rDNA in comparison with the standard ladder are represented in fig. 4A and fig. 4B, respectively. The obtained sequence of 985 base pairs was submitted to the gene bank with accession number MN235945. Finally, to validate the reproducibility, the phylogenetic tree was constructed by the bootstrap analysis method using MegAlign Pro (DNASTAR Lasergene) software (fig. 5A). The colony of *Amycolatopsis* sp. strain MN235945 was having an ovoid structure with a rough surface and was monosporous (fig. 5B). Likewise, the biosynthesis of AgNPs from *Streptomyces rochei* MHM13[13], where the potent isolate was identified based on 16S rRNA gene sequencing followed by the analysis of phylogenetic tree of the isolate along with the most similar sequences obtained *via* BLASTn.

The antagonistic activity of synthesized AgNPs were investigated against both bacteria and fungi organisms using well diffusion method (fig. 6). The results documented that among the selected bacterial pathogens, *Escherichia coli* exhibited 19 mm, 19 mm, 21 mm and 22 mm of inhibition zones for 25, 50, 75, and 100 µl of AgNPs suspension; whereas, among the fungal pathogens, *Alternaria alternata* was found to be the most sensitive with inhibition zones of 18 mm, 19 mm, 19 mm, and 20 mm for 25, 50, 75, and 100 µl of AgNPs suspension, respectively. However, *Staphylococcus aureus* and *Fusarium oxysporum* were found to be least sensitive to the biosynthesized AgNPs among the tested microbial pathogens. The ability of the AgNPs to inhibit all tested organisms suggested that, these nanoparticles contained potential antimicrobial activity against infectious pathogens. They also suggested that the AgNPs attach to the microbial cell wall and interact with lipopolysaccharides and disrupt them. The AgNPs binds to enzymes, proteins, and DNA upon entering into the bacterial cell and lead to cell death by disrupting the cellular biochemical reactions and DNA replication mechanism of the microbial pathogens[37,38].

The synthesized AgNPs exhibited considerable MIC and MBC values against all the tested bacterial pathogens by inhibiting the growth of pathogenic bacteria even at low concentrations. The biogenic AgNPs showed significant bactericidal activity against pathogens and the results were showed in Table 1. Similar results from previous studies on MIC and MBC activities of microbial mediated AgNPs reported that the biological AgNPs displayed high inhibitory activity against bacterial pathogens even at low concentrations. They concluded that the AgNPs with smaller sizes provide a larger surface area for interaction with the microbial cell membrane, adding to the alterations in some primary functions of bacteria, such as permeability and cell respiration[39,40].

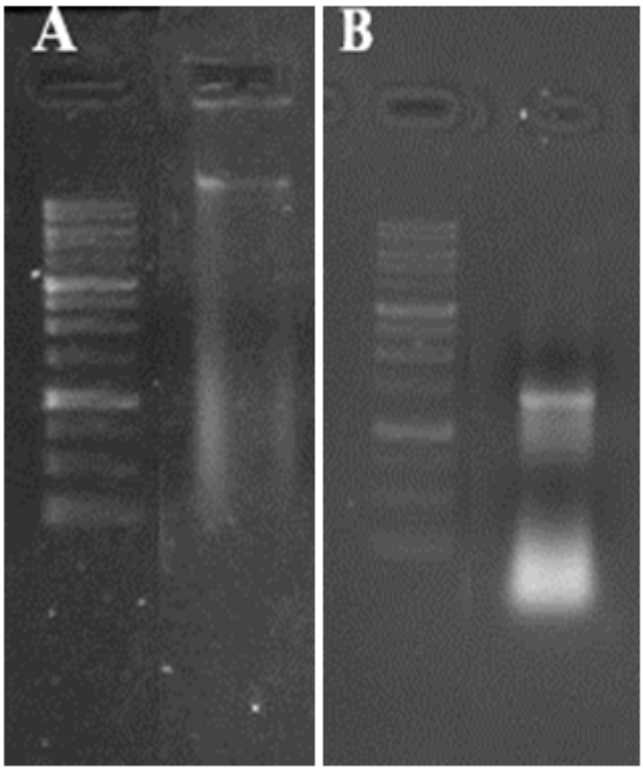

Fig. 4: Agarose gel electrophoresis image of *Amycolatopsis* sp. strain MN235945; (A) Genomic 16S rRNA gene with 1 kilobase ladder and (B) Amplified 16S rRNA gene with 1 kilobase ladder.

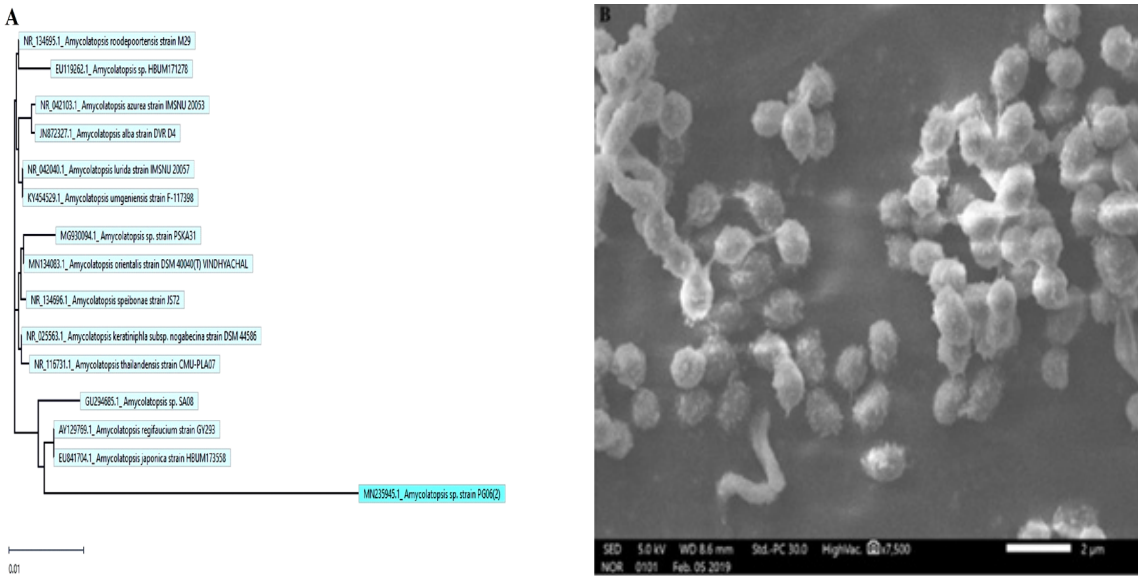

Fig. 5: Genotypic and Morphological characterization, (A) Phylogenetic tree and (B) SEM Image shows spore formation of *Amycolatopsis* sp. strain MN235945

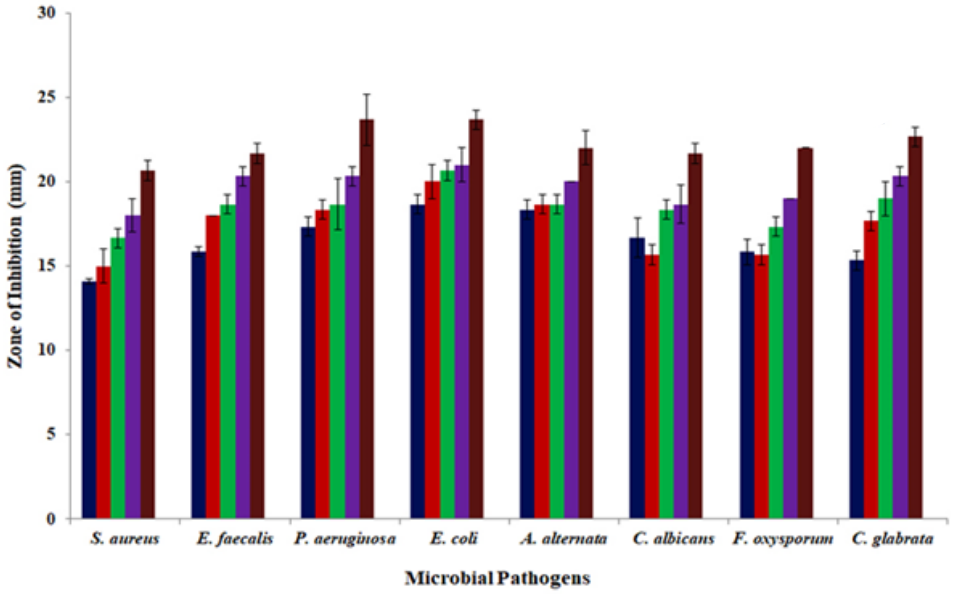

Fig. 6: Antimicrobial activity of AgNPs synthesized by *Amycolatopsis* sp. strain MN235945 against pathogenic microorganisms; Note: ( ): 25 µL of AgNPs; ( ):50 µL of AgNPs; ( ): 75 µL of AgNPs; ( ): 100 µL of AgNPs; ( ): +ve control; ( ): -ve control

TABLE 1: MIC AND MBC VALUES OF AGNPS SYNTHESIZED BY *Amycolatopsis* sp. STRAIN MN235945 AGAINST PATHOGENIC MICROORGANISMS

S NO.	Name of the Pathogen	Std. (µg/ml)	MIC (µg/ml)	MBC (µg/ml)
1	*Staphylococcus aureus*	10±0.5	128±1.0	128±1.0
2	*Enterococcus faecalis*	7±0.5	64±0.57	64±0.57
3	*Pseudomonas aeruginosa*	10±0.76	32±1.0	64±0.76
4	*Escherichia coli*	5±0.36	48±1.52	48±1.0

Note: *Values are in mean three replicates±SD

In vitro anticancer activity of AgNPs against HeLa and MCF-7 cell lines and the morphological changes of HeLa and MCF-7 cell lines on the addition of different concentrations of AgNPs and standard drug camptothecin were recorded using a confocal microscope. The synthesized AgNPs had dose-dependent cytotoxic effects on HeLa and MCF-7 cells *in vitro* (fig. 7A- fig. 7G and fig. 8A-fig. 8G) with exhibiting IC_{50} concentrations of 81.12 µg/ml and 235.45 µg/ml against HeLa and MCF-7 cells, respectively. Similarly, previous studies conducted on the anticancer activities of AgNPs against selected cell lines reported that the AgNPs showed dose-dependent activity. The AgNPs treated cells were different from the untreated cells in cell shape, size, and other morphological details and the morphological changes in the cells including rounding or shrinking at varying degrees was a clear indication of cytotoxicity[41,42].

The ROS production was coupled with AgNPs and potentially induced cell death in HeLa and MCF-7 cell lines and untreated cells (fig. 9A- fig. 9G and fig. 10A-fig. 10G) after treatment of AgNPs at different time intervals from 0 to 120 min. The notable increase in the ROS expression level was observed with increase in concentration of AgNPs through elevating fluorescent intensity and the appearance of dissembled gaps between neighbouring cells were characteristics of apoptosis. Whereas, the fluorescent green coloured cells represented the presence of AgNPs absorbed by the cancer cells. According to the previous reports, ROS are free radicals that play a vital role in the living system by causing cell damage and cell death. AgNPs treated cells were different from the untreated cells in case of cell shape, size and other morphological details. The treated cells were somewhat granular shaped with less well-defined colony morphology and the rapidly increased ROS generation was due to the nature of surface, size, shape, and intensity of AgNPs. The overproduction of ROS induces apoptosis in several types of cancers, and cell death occurs due to an imbalance between pro and anti-oxidants levels inside the tumour cells[43-45].

The present work illustrated an environmental friendly and cost effective synthesis procedure of small sized AgNPs using marine Actinomycete *Amycolatopsis* sp. strain MN235945. UV-Vis observation of *Amycolatopsis* sp. AgNPs shown absorption maximum at 417 nm, FTIR analysis revealed the presence of biomolecules involved in the capping and stabilization, and TEM data confirmed that the particles were polydispersed and spherical in shape with 19.40 nm being the smallest particle size. The EDX confirmed the elemental analysis of AgNPs; whereas, zeta potential of biosynthesized AgNPs was found at -34.8 mV and the crystalline nature was determined by XRD analysis. The microbial synthesized AgNPs showed increased antimicrobial and anticancer activity with increase in concentration. Based on these findings, the *Amycolatopsis* sp. strain MN235945 AgNPs may be used for valuable applications in various fields such as medicine, clinical and could also be used as anticancer agents after successful clinical test and other *in vivo* studies.

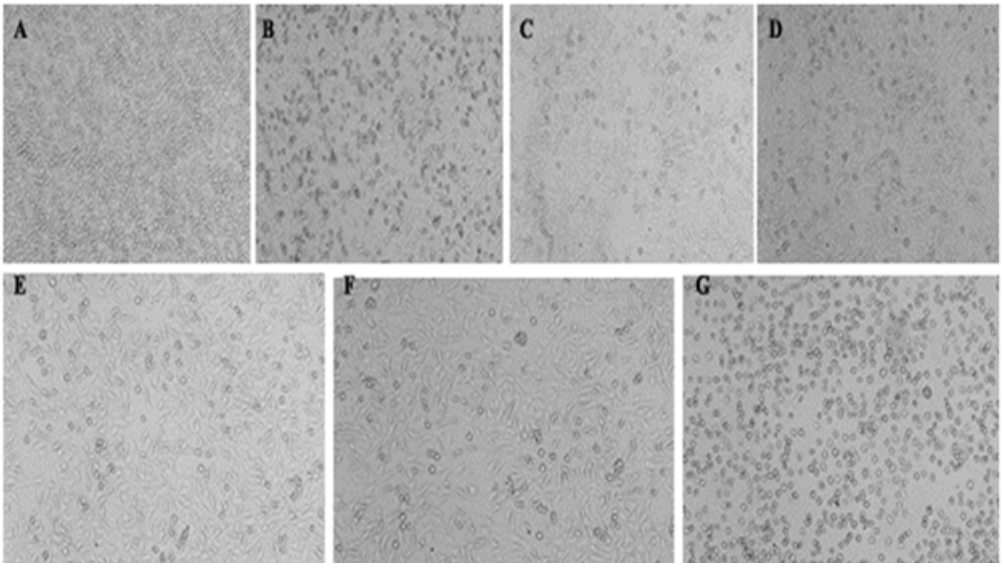

Fig. 7: MTT anticancer activity of *Amycolatopsis* sp. strain MN235945 AgNPs on HeLa cell line; (A) Untreated; (B) Standard; (C) 6.25µg/ml; (D) 12.5 µg/ml; (E) 25 µg/ml; (F) 50 µg/ml and (G) 100 µg/ml of AgNPs treatment

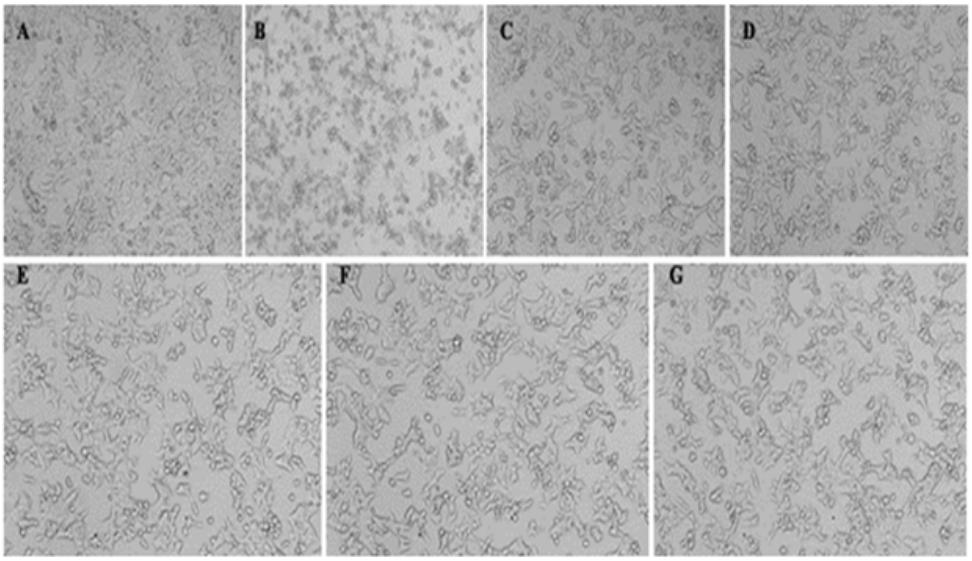

Fig. 8: MTT anticancer activity of *Amycolatopsis* sp. strain MN235945 AgNPs on MCF-7 cell line; (A) Untreated; (B) Standard; (C) 6.25µg/ml; (D) 12.5 µg/ml; (E) 25 µg/ml; (F) 50 µg/ml and (G) 100 µg/ml of AgNPs treatment

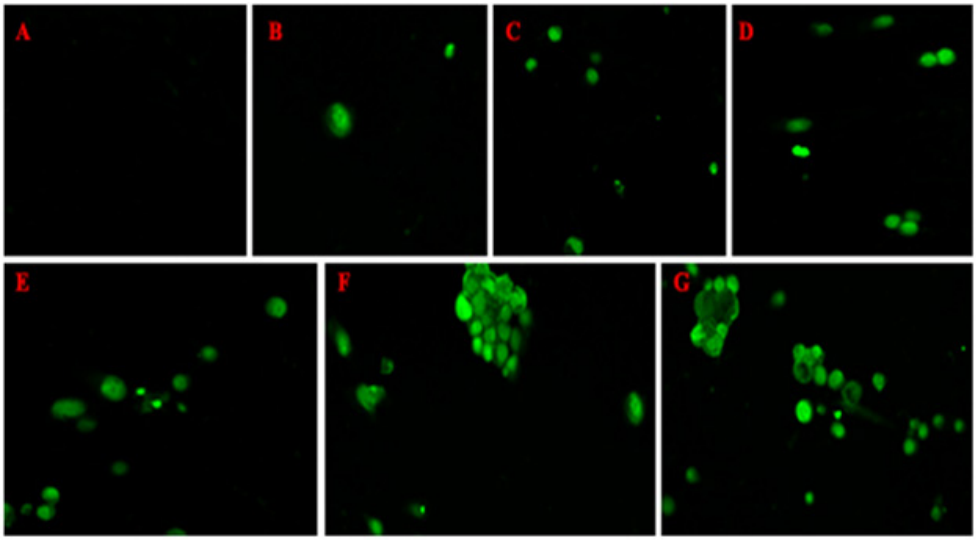

Fig. 9: ROS-mediated apoptosis assay of *Amycolatopsis* sp. strain MN235945 AgNPs on HeLa cell line, (A) 0 min; (B) 5 min; (C) 15 min; (D) 30 min; (E) 60 min; (F) 90 min and (G) 120 min of treatment time

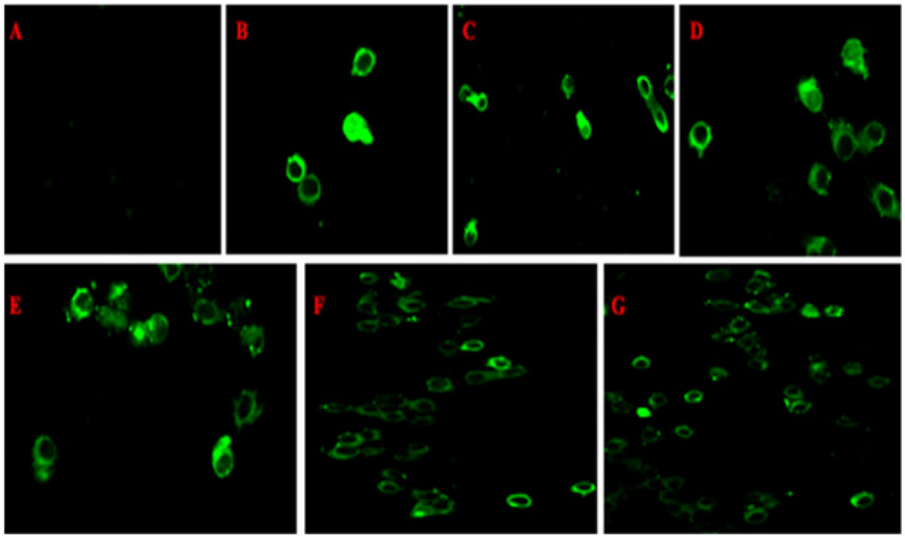

Fig. 10: ROS-mediated apoptosis assay of *Amycolatopsis* sp. strain MN235945 AgNPs on MCF7 cell line, (A) 0 min; (B) 5 min; (C) 15 min; (D) 30 min; (E) 60 min; (F) 90 min and (G) 120 min of treatment time

Acknowledgments:

The authors would like to thank University Scientific Instrumentation Center (USIC), Karnatak University Dharwad, for extending instrumentation facilities and the work was supported by the University Research Scholarship (URS), Karnatak University, Dharwad .

Author contributions:

SN designed the concept and supervised the experiments. PSS carried out experimental analysis and wrote the manuscript. MPB wrote and edited the manuscript.

Statement on the welfare of animals:

This article does not contain any studies with human participants or animals performed by any of the authors.

Informed consent:

Informed consent was obtained from all individual participants included in the study.

Conflicts of interest:

The authors declare no conflict of interest.

REFERENCES

1. Park W, Heo YJ, Han DK. New opportunities for nanoparticles in cancer immunotherapy. Biomater Res 2018;22(1):1-10.
2. Madhankumar R, Sivasankar P, Kalaimurugan D, Murugesan S. Antibacterial and larvicidal activity of silver nanoparticles synthesized by the leaf extract of *Andrographis serpyllifolia* wight. J Clust Sci 2020;31(4):719-26.
3. Singh L, Kruger HG, Maguire GE, Govender T, Parboosing R. The role of nanotechnology in the treatment of viral infections. Ther Adv Infect Dis 2017;4(4):105-31.
4. Anitha R, Ramesh KV, Ravishankar TN, Kumar KS, Ramakrishnappa T. Cytotoxicity, antibacterial and antifungal activities of ZnO nanoparticles prepared by the *Artocarpus gomezianus* fruit mediated facile green combustion method. J Sci Adv Mater Dev 2018;3(4):440-51.
5. Kaul S, Gulati N, Verma D, Mukherjee S, Nagaich U. Role of nanotechnology in cosmeceuticals: A review of recent advances. J Pharm 2018;2018:3420204.
6. Mihai MM, Dima MB, Dima B, Holban AM. Nanomaterials for wound healing and infection control. Materials 2019;12(13):2176.
7. Eswari JS, Dhagat S, Mishra P. Biosurfactant assisted silver nanoparticle synthesis: A critical analysis of its drug design aspects. Adv Nat Sci Nanosci Nanotechnol 2018;9(4):045007.
8. Kumari R, Saini AK, Kumar A, Saini RV. Apoptosis induction in lung and prostate cancer cells through silver nanoparticles synthesized from *Pinus roxburghii* bioactive fraction. JBIC J Biol Inorg Chem 2020;25(1):23-37.
9. Katsuki S, Matoba T, Koga JI, Nakano K, Egashira K. Anti-inflammatory nanomedicine for cardiovascular disease. Front Cardiovasc Med 2017;4:87.
10. Martirosyan A, Schneider YJ. Engineered nanomaterials in food: Implications for food safety and consumer health. Int J Environ Res Public Health 2014;11(6):5720-50.
11. Sharma C, Dhiman R, Rokana N, Panwar H. Nanotechnology: An untapped resource for food packaging. Front Microbiol 2017;8:1735.
12. Nakamura S, Sato M, Sato Y, Ando N, Takayama T, Fujita M, *et al.* Synthesis and application of silver nanoparticles (Ag NPs) for the prevention of infection in healthcare workers. Int J Mol Sci 2019;20(15):3620.
13. Abd-Elnaby HM, Abo-Elala GM, Abdel-Raouf UM, Hamed MM. Antibacterial and anticancer activity of extracellular synthesized silver nanoparticles from marine *Streptomyces rochei* MHM13. Egypt J Aquat Res 2016;42(3):301-12.
14. Devi LS, Joshi SR. Ultrastructures of silver nanoparticles biosynthesized using endophytic fungi. J Microsc Ultrastruct 2015;3(1):29-37.
15. Sarsar V, Selwal MK, Selwal KK. Biofabrication, characterization and antibacterial efficacy of extracellular silver nanoparticles using novel fungal strain of *Penicillium atramentosum* KM. J Saudi Chem Soc 2015;19(6):682-8.
16. Shaker MA, Shaaban MI. Synthesis of silver nanoparticles with antimicrobial and anti-adherence activities against multidrug-resistant isolates from *Acinetobacter baumannii*. J Taibah Univ Med Sci 2017;12(4):291-7.
17. Sowani H, Mohite P, Munot H, Shouche Y, Bapat T, Kumar AR, *et al.* Green synthesis of gold and silver nanoparticles by an actinomycete *Gordonia amicalis* HS-11: Mechanistic aspects and biological application. Process Biochem 2016;51(3):374-83.
18. Baltazar-Encarnación E, Escárcega-González CE, Vasto-Anzaldo XG, Cantú-Cárdenas ME, Morones-Ramírez JR. Silver nanoparticles synthesized through green methods using *Escherichia coli* top 10 (Ec-Ts) growth culture medium exhibit antimicrobial properties against nongrowing bacterial strains. J Nanomater 2019;2019.
19. Mohd Yusof H, Abdul Rahman NA, Mohamad R, Zaidan UH. Microbial mediated synthesis of silver nanoparticles by *Lactobacillus plantarum* TA4 and its antibacterial and antioxidant activity. Appl Sci 2020;10(19):6973.
20. Senthilkumar P, Santhosh Kumar DS, Sudhagar B, Vanthana M, Parveen MH, Sarathkumar S, *et al.* Seagrass-mediated silver nanoparticles synthesis by *Enhalus acoroides* and its α-glucosidase inhibitory activity from the Gulf of mannar. J Nanostruct Chem 2016;6(3):275-80.
21. Wink JM, Kroppenstedt RM, Ganguli BN, Nadkarni SR, Schumann P, Seibert G, *et al.* Three new antibiotic producing species of the genus *Amycolatopsis*, *Amycolatopsis balhimycina* sp. nov., *A. tolypomycina* sp. nov., *A. vancoresmycina* sp. nov., and description of *Amycolatopsis keratiniphila* subsp. *keratiniphila* subsp. nov. and *A. keratiniphila* subsp. *nogabecina* subsp. nov. System Appl Microbiol 2003;26(1):38-46.
22. Bray F, Ferlay J, Soerjomataram I, Siegel RL, Torre LA, Jemal A. Global cancer statistics 2018: GLOBOCAN estimates of incidence and mortality worldwide for 36 cancers in 185 countries. CA Cancer J Clin 2018;68(6):394-424.
23. Moussavou G, Kwak DH, Obiang-Obonou BW, Ogandaga Maranguy CA, Dinzouna-Boutamba SD, Lee DH, *et al.* Anticancer effects of different seaweeds on human colon and breast cancers. Mar Drugs 2014;12(9):4898-911.
24. Rajeshkumar S. Anticancer activity of eco-friendly gold nanoparticles against lung and liver cancer cells. J Genet Eng Biotechnol 2016;14(1):195-202.

25. Nagajyothi PC, Muthuraman P, Sreekanth TV, Kim DH, Shim J. Green synthesis: *In vitro* anticancer activity of copper oxide nanoparticles against human cervical carcinoma cells. Arab J Chem 2017;10(2):215-25.
26. Barai AC, Paul K, Dey A, Manna S, Roy S, Bag BG, *et al.* Green synthesis of *Nerium oleander*-conjugated gold nanoparticles and study of its *in vitro* anticancer activity on MCF-7 cell lines and catalytic activity. Nano Converg 2018;5(1):1-10.
27. Husseiny SM, Salah TA, Anter HA. Biosynthesis of size controlled silver nanoparticles by Fusarium oxysporum, their antibacterial and antitumor activities. Beni-Suef Univ J Basic Appl Sci 2015;4(3):225-31.
28. Desai PP, Prabhurajeshwar C, Chandrakanth KR. Hydrothermal assisted biosynthesis of silver nanoparticles from *Streptomyces* sp. GUT 21 (KU500633) and its therapeutic antimicrobial activity. J Nanostruct Chem 2016;6(3):235-46.
29. Manivasagan P, Venkatesan J, Senthilkumar K, Sivakumar K, Kim SK. Biosynthesis, antimicrobial and cytotoxic effect of silver nanoparticles using a novel *Nocardiopsis* sp. MBRC-1. Biomed Res Int 2013;2013:287638.
30. Dhanaraj S, Thirunavukkarasu S, John HA, Pandian S, Salmen SH, Chinnathambi A, *et al.* Novel marine *Nocardiopsis dassonvillei*-DS013 mediated silver nanoparticles characterization and its bactericidal potential against clinical isolates. Saudi J Biol Sci 2020;27(3):991-5.
31. Kamel Z, Saleh M, El Namoury N. Biosynthesis, characterization, and antimicrobial activity of silver nanoparticles from actinomycetes. Res J Pharm Biol Chem Sci 2016;7(1):119-27.
32. Avilala J, Golla N. Antibacterial and antiviral properties of silver nanoparticles synthesized by marine actinomycetes. Int J Pharm Sci Res 2019;10(3):1223-8.
33. John MS, Nagoth JA, Ramasamy KP, Mancini A, Giuli G, Natalello A, *et al.* Synthesis of bioactive silver nanoparticles by a *Pseudomonas* strain associated with the antarctic psychrophilic protozoon *Euplotes focardii*. Mar Drugs 2020;18(1):38.
34. Jayaprakash N, Vijaya JJ, Kaviyarasu K, Kombaiah K, Kennedy LJ, Ramalingam RJ, *et al.* Green synthesis of Ag nanoparticles using Tamarind fruit extract for the antibacterial studies. J Photochem Photobiol B 2017;169:178-85.
35. Vijayabharathi R, Sathya A, Gopalakrishnan S. Extracellular biosynthesis of silver nanoparticles using *Streptomyces griseoplanus* SAI-25 and its Antifungal activity against *Macrophomina phaseolina*, the charcoal rot pathogen of sorghum. Biocatal Agric Biotechnol 2018;14:166-71.
36. Salem SS, El-Belely EF, Niedbała G, Alnoman MM, Hassan SE, Eid AM, *et al.* Bactericidal and *in vitro* cytotoxic efficacy of silver nanoparticles (Ag-NPs) fabricated by endophytic actinomycetes and their use as coating for the textile fabrics. Nanomaterials 2020;10(10):2082.
37. Prakasham RS, Kumar BS, Kumar YS, Kumar KP. Production and characterization of protein encapsulated silver nanoparticles by marine isolate *Streptomyces parvulus* SSNP11. Indian J Microbiol 2014;54(3):329-36.
38. Sujatha J, Suriya P, Rajeshkumar S. Biosynthesis and characterization of silver nanoparticles by actinomycetes isolated from agriculture field and its application on antimicrobial activity. Res J Pharm Tech 2017;10(6):1963-8.
39. Al-Dhabi NA, Ghilan AK, Arasu MV, Duraipandiyan V. Green biosynthesis of silver nanoparticles produced from marine *Streptomyces* sp. Al-Dhabi-89 and their potential applications against wound infection and drug resistant clinical pathogens. J Photochem Photobiol B 2018;189:176-84.
40. Mohamedin A, El-Naggar NE, Shawqi Hamza S, Sherief AA. Green synthesis, characterization and antimicrobial activities of silver nanoparticles by Streptomyces viridodiastaticus SSHH-1 as a living nanofactory: Statistical optimization of process variables. Curr Nanosci 2015;11(5):640-54.
41. Bhat M, Chakraborty B, Kumar RS, Almansour AI, Arumugam N, Kotresha D, *et al.* Biogenic synthesis, characterization and antimicrobial activity of *Ixora brachypoda* (DC) leaf extract mediated silver nanoparticles. J King Saud Univ Sci 2021;33(2):101296.
42. Rathod D, Golinska P, Wypij M, Dahm H, Rai M. A new report of *Nocardiopsis valliformis* strain OT1 from alkaline Lonar crater of India and its use in synthesis of silver nanoparticles with special reference to evaluation of antibacterial activity and cytotoxicity. Med Microbiol Immunol 2016;205(5):435-47.
43. Nayaka SR, Chakraborty BI, Pallavi SS, Bhat MP, Shashiraj KN, Ghasti BH. Synthesis of biogenic silver nanoparticles using *Zanthoxylum rhetsa* (Roxb.) DC seed coat extract as reducing agent and *in vitro* assessment of anticancer effect on A549 lung cancer cell line. Int J Pharm Res 2020;12(3):302-14.
44. Zhu B, Li Y, Lin Z, Zhao M, Xu T, Wang C, *et al.* Silver nanoparticles induce HePG-2 cells apoptosis through ROS-mediated signaling pathways. Nanoscale Res Lett 2016;11(1):198.
45. Barcińska E, Wierzbicka J, Zauszkiewicz-Pawlak A, Jacewicz D, Dabrowska A, Inkielewicz-Stepniak I. Role of oxidative and nitro-oxidative damage in silver nanoparticles cytotoxic effect against human pancreatic ductal adenocarcinoma cells. Oxid Med Cell Longev 2018;2018:8251961.